A&A 648, C2 (2021)
https://doi.org/10.1051/0004-6361/201834565e

Astronomy & Astrophysics

Exploring He II λ1640 emission line properties at $z \sim 2$–4 (*Corrigendum*)

Themiya Nanayakkara[1], Jarle Brinchmann[1,2], Leindert Boogaard[1], Rychard Bouwens[1], Sebastiano Cantalupo[3], Anna Feltre[4,5], Wolfram Kollatschny[6], Raffaella Anna Marino[3], Michael Maseda[1], Jorryt Matthee[3], Mieke Paalvast[1], Johan Richard[4], and Anne Verhamme[7]

[1] Leiden Observatory, Leiden University, PO Box 9513, 2300 RA Leiden, The Netherlands
e-mail: themiyananayakkara@gmail.com
[2] Instituto de Astrofisica e Ciencias do Espaco, Universidade do Porto, CAUP, Rua das Estrelas, 4150-762 Porto, Portugal
[3] ETH Zurich, Department of Physics, HIT J31.5, Wolfgang-Pauli-Strasse 27, 8093 Zurich, Switzerland
[4] Univ. Lyon, Univ. Lyon1, ENS de Lyon, CNRS, Centre de Recherche Astrophysique de Lyon (CRAL) UMR 5574, 69230 Saint-Genis-Laval, France
[5] Scuola Internazionale Superiore di Studi Avanzati (SISSA), Via Bonomea 265, 34136 Trieste, Italy
[6] Institut für Astrophysik, Universität Göttingen, Friedrich-Hund Platz 1, 37077 Göttingen, Germany
[7] Observatoire de Genève, Université de Genève, 51 Ch. des Maillettes, 1290 Versoix, Switzerland

A&A 624, A89 (2019), https://doi.org/10.1051/0004-6361/201834565

ABSTRACT

Key words. galaxies: ISM – galaxies: star formation – galaxies: evolution – galaxies: high-redshift – errata, addenda

Due to an error introduced to the equivalent width measuring code during the refereeing process, the final published equivalent widths (EWs) were artificially elevated. Table 3 and Fig. 10 have been updated with the correct values. The He II λ1640 EW values still show an enhancement compared to the values predicted by the models. Our final conclusions therefore remain unchanged due to this update.

Table 3. EWs of the MUSE He II λ1640 sample used in this analysis.

ID	He II λ1640		C III]1907		C III]1909		O III]1661		O III]1666		Si III]1883		Si III]1892	
	EW	ΔEW	EW	ΔEW	EW	ΔEW	EW	ΔEW	EW	ΔEW	EW	ΔEW	EW	ΔEW
1024	3.1	0.6	6.0	0.9	4.0	0.5	1.3	0.6	2.8	0.6	3.6	0.7	3.2	1.1
1036	3.0	1.1	12.4	0.8	8.5	1.0	2.1	0.7	4.8	0.7	4.6	0.6	2.5	0.8
1045	3.6	0.9	11.5	1.2	6.3	1.1	3.2	0.8	4.6	0.8	4.1	0.7	3.8	0.8
1079	8.2	2.0	21.3	1.8	14.4	1.5	3.6	1.1	7.2	1.4	7.3	1.9	3.0	1.4
1273	10.3	−99.0	7.2	−99.0	12.4	−99.0	10.2	−99.0	10.1	−99.0	14.5	−99.0	7.0	−99.0
3621	4.8	0.8	7.1	0.8	3.0	0.8	2.1	0.5	3.8	0.5	2.9	0.5	4.1	0.7
87	3.2	0.4	5.7	0.5	5.0	0.5	1.5	0.5	4.3	0.5	4.5	0.7	2.2	0.7
109	10.7	2.2	–	–	–	–	9.7	1.8	37.2	4.3	–	–	–	–
144	17.9	2.4	28.9	3.1	20.2	3.8	8.8	1.4	16.9	1.9	7.7	1.9	3.0	1.8
97	24.7	−99.0	–	–	–	–	5.1	−99.0	1.3	−99.0	–	–	–	–
39	26.9	3.5	18.6	−99.0	12.0	−99.0	8.5	2.4	6.3	2.0	39.4	−99.0	23.3	−99.0
84	50.3	−99.0	10.4	−99.0	0.3	−99.0	1.7	−99.0	6.9	−99.0	6.6	−99.0	12.0	−99.0
161	9.1	2.6	0.7	0.6	1.5	0.7	0.2	0.7	0.2	0.4	0.0	0.4	0.4	0.6

Notes. All EWs are in Å. EW errors were obtained from bootstrap resampling of the spectrum and account for the uncertainty in continuum fitting. If a line is not covered by the spectral range of MUSE, the EW is shown by a long dash. If a line is covered but the continuum level around the considered line is below the error level, the ΔEW is shown by a long dash. In these cases, the EW was computed assuming that the continuum level equals the noise level, and the EW presented should be considered as a lower limit.

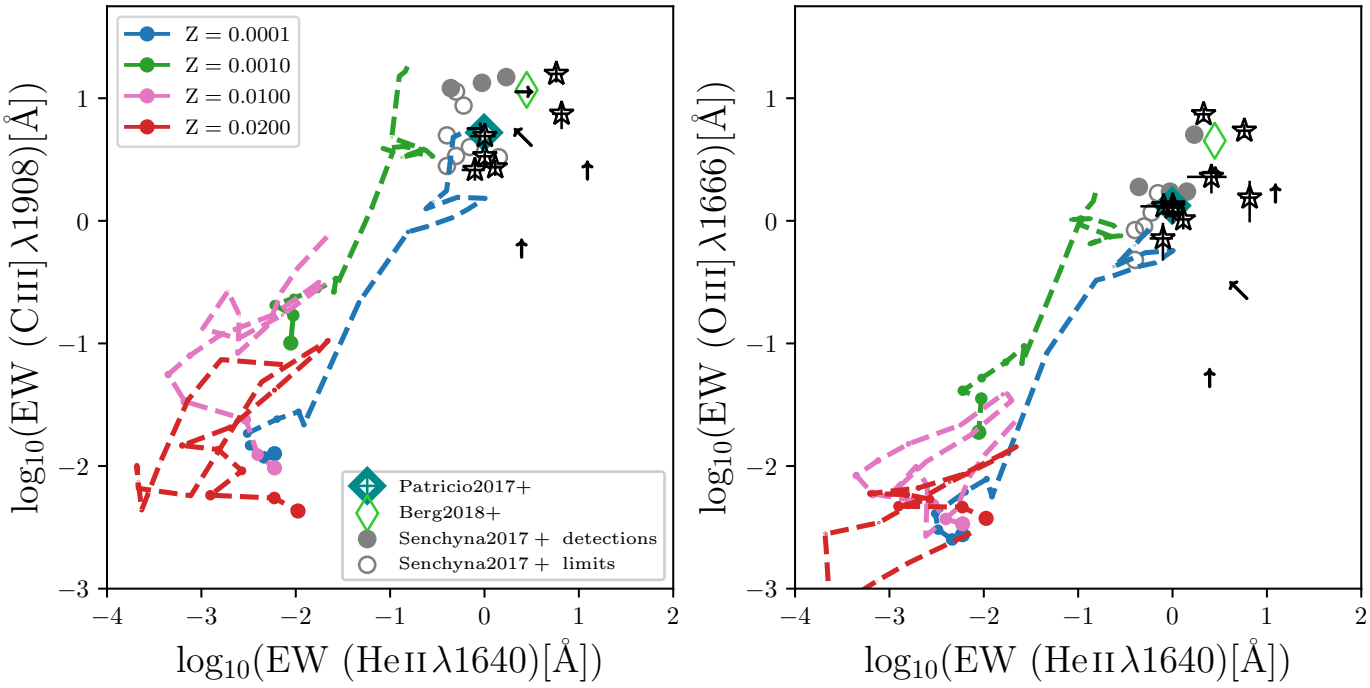

Fig. 10. EW comparison of the MUSE He II λ1640 sample using BPASS stellar population models. *Left*: C III]λ1907+C III]λ1909 EW vs. He II λ1640 EW. *Right*: O III]λ1666 EW vs. He II λ1640 EW. Galaxies with $S/N \geq 2.5$ are shown by stars, and others are shown as lower limits to the EW as triangles. We compare our observed EWs with model tracks from the Xiao et al. (2018) BPASS binary tracks. Models were computed for a $\log_{10}(n_H) = 1.0$ and $U_s = -1.5$ at different metallicities between 2 $Z_\odot$ to 1/200th $Z_\odot$. The size of the symbols increases with time. EWs from the literature are also shown for comparison.

References

Xiao, L., Stanway, E. R., & Eldridge, J. J. 2018, MNRAS, 477, 904